

1 **Prognostic significance of GAD1 overexpression in patients with resected lung**

2 **adenocarcinoma**

3

4 Mitsuhiro Tsuboi MD¹, Kazuya Kondo, MD, PhD², Kiyoshi Masuda, MD, PhD^{3,4}, Shoichiro
5 Tange, PhD³, Koichiro Kajiura, MD, PhD¹, Tomohiro Kohmoto³, Hiromitsu Takizawa, MD,
6 PhD¹, Issei Imoto, MD, PhD^{3, 5, 6}, and Akira Tangoku, MD, PhD¹

7 ¹Department of Thoracic, Endocrine Surgery and Oncology, Institute of Biomedical Sciences,
8 Tokushima University Graduate School, Tokushima, Japan

9 ²Department of Oncological Medical Services, Institute of Biomedical Sciences, Tokushima
10 University Graduate School, Tokushima, Japan

11 ³Department of Human Genetics, Institute of Biomedical Sciences, Tokushima University
12 Graduate School, Tokushima, Japan

13 ⁴Kawasaki Medical School, Kurashiki, Japan

14 ⁵Division of Molecular Genetics, Aichi Cancer Center Research Institute, Nagoya, Japan

15 ⁶Department of Cancer Genetics, Nagoya University Graduate School of Medicine, Nagoya
16 466-8550, Japan

17

18 Corresponding author

19 Kazuya Kondo, MD, PhD

20 Department of Oncological Medical Services, Institute of Biomedical Sciences, Tokushima
21 University Graduate School, Tokushima, Japan

22 3-18-15 Kuramotocho, Tokushima City, Tokushima Pref. 770-8503, Japan

23 E-mail: kzykondo@tokushima-u.ac.jp

24

25 **ABSTRACT**

26

27 **Background and Objectives:** In a previous genome-wide screening, we identified
28 hypermethylated CpG islands around *glutamate decarboxylase 1 (GAD1)* in lung
29 adenocarcinoma (LADC). In this study, we aimed to investigate the methylation and expression
30 status of GAD1 and its prognostic value in patients with LADC.

31

32 **Methods:** *GAD1* methylation and mRNA expression status were analyzed using 33 tumorous
33 and paired non-tumorous LADC samples and publicly available datasets. The prognostic value
34 of GAD1 overexpression was investigated using publicly available datasets of mRNA levels and
35 162 cases of LADC by immunohistochemistry.

36

37 **Results:** The methylation and mRNA expression levels of GAD1, each having a positive
38 correlation, were significantly higher in LADC tumors than in paired non-tumorous tissues.
39 LADC patients with higher GAD1 mRNA expression showed significantly poorer prognosis for
40 overall survival in publicly available datasets. Higher immunoreactivity of GAD1 was
41 significantly associated with the pathological stage, pleural invasion, lymph vessel invasion, and
42 poorer prognosis for cancer-specific and disease-free survival. Multivariate analysis revealed
43 that GAD1 protein overexpression is an independent prognosticator for disease-free survival.

44

45 **Conclusions:** GAD1 mRNA and protein expression levels were significant prognostic factors in
46 LADC, suggesting that they might be useful biomarkers to stratify patients with worse clinical
47 outcome after resection.

48

49 **Keywords:** GAD1, lung adenocarcinoma, expression, prognosis, DNA methylation

50

51 **1. INTRODUCTION**

52 Lung adenocarcinoma (LADC) is the predominant histological subtype of lung cancer and has
53 the highest mortality rate worldwide [1, 2]. Although progress in the treatment of LADC has
54 improved short-term survival, the impacts on long-term survival remain modest [3]. Therefore,
55 a better understanding of the mechanisms of LADC tumor progression is needed and useful
56 prognostic molecular markers for accurately predicting the clinical outcomes of LADC are of
57 great clinical significance.

58 To identify genes in the tumor that are specifically methylated at an early-stage of LADC,
59 we had previously performed a genome-wide screening of aberrantly methylated CpG islands
60 (CGIs) using paired tumorous and non-tumorous tissues of early-stage LADC, and identified
61 *TRIM58* as a novel candidate tumor-suppressor gene for this disease [4]. Through this screening,
62 the glutamate decarboxylase 1 gene (*GADI*) was found to be nearby hypermethylated CGIs in
63 LADC. Because paradoxical hypermethylation-associated overexpression of *GADI* was
64 reported recently in colorectal and liver cancers [5] and *GADI* overexpression has been reported
65 in various neoplastic tissues, such as oral, nasopharyngeal, colorectal, liver, and gastric cancers
66 [5-9], we focused on *GADI* as a potential LADC-related gene in the present study. Moreover,
67 the methylation and expression status and clinicopathological significance of *GADI* in LADC
68 tumorigenesis have also not been examined previously.

69 Therefore, in the present study, we investigated the DNA methylation and mRNA and
70 protein expression status of *GADI* in resected LADC tumors. Moreover, we assessed the
71 prognostic significance of *GADI* expression in LADC using our tumor panel and publicly
72 available datasets.

73

74 **2. MATERIALS AND METHODS**

75 *2.1. Selection of candidate CGI*

76 Previously obtained Human Methylation 450K array-based methylation screening data of 12
77 paired tumorous/non-tumorous stage-I LADC sample sets from patients (6 smokers and 6 never-
78 smokers) who underwent surgery at Tokushima University Hospital (Tokushima, Japan)
79 between April 1999 and March 2015 were reevaluated (Supplementary Table S1) [4].

80

81 *2.2. Patients and tissue samples*

82 We included tumors and non-tumorous tissues of LADC that were surgically resected at
83 Tokushima University Hospital between April 1999 and November 2013 for additional analyses.
84 No patients had been administered preoperative radiation, chemotherapy, or immunotherapy.
85 For pyrosequencing-based methylation analysis and real-time PCR-based expression analysis,
86 33 LADC samples were used (Supplementary Table S2). For immunohistochemical staining,
87 162 LADC samples were used (Supplementary Table S3). The mean follow-up duration for the
88 162 patients with LADC was 48 months (range, 0.6–147 months), with 45 recurrences (27.8%)
89 and 34 deaths (21.0%) among the patients. Tumor staging was determined based on the seventh
90 tumor-node-metastasis (TNM) classification for lung cancer [10]. The tumors were classified
91 according to the predominant histological subtype, as proposed by the 2015 WHO classification
92 [11].

93 This study was performed in accordance with the principles outlined in the Declaration of
94 Helsinki. The ethics committee of Tokushima University Hospital approved the study (approval
95 number 3048), and formal written consent was obtained from all patients or their
96 representatives.

97

98 *2.3. DNA and RNA preparation and bisulfite conversion of genomic DNA*

99 DNA and RNA were extracted using standard methods. Bisulfite conversion of DNA was
100 conducted using the EpiTect Bisulfite Kit (QIAGEN GmbH, Hilden, Germany) following the
101 manufacturer's instructions.

102

103 *2.4. Bisulfite pyrosequencing*

104 Bisulfite-treated genomic DNA was amplified using a set of primers designed with PyroMark
105 Assay Design Software version 2.0.01.15 (QIAGEN GmbH, Supplementary Table S4). The
106 target region for sequencing began 10 nucleotides (nt) before and ended 26 nt after cg15126544.
107 PCR product pyrosequencing and methylation quantification were performed with sequencing
108 primers using the PyroMark 24 Pyrosequencing System, version 2.0.6 (QIAGEN GmbH),
109 according to the manufacturer's instructions.

110

111 *2.5. Real-time quantitative reverse-transcription polymerase chain reaction (rqRT-PCR)*

112 Complementary DNA was generated from isolated total RNA using the PrimeScript II 1st strand
113 cDNA Synthesis Kit (TaKaRa, Shiga, Japan). rqRT-PCR was performed using KAPA PROBE
114 FAST qPCR Kits (Kapa Biosystems, Wilmington, MA, USA) and TaqMan Gene Expression
115 Assays (Thermo Fisher Scientific, Waltham, MA, USA; Supplementary Table S4) according to
116 the manufacturers' instructions. *GAPDH* mRNA levels were used as internal controls for
117 normalization. Relative expression of *GADI* mRNA was calculated using Human Lung Total
118 RNA (TaKaRa) as a normal lung control.

119

120 *2.6. Data mining in bioinformatics*

121 Available RNA sequencing data (IlluminaHiSeq_RNASeqV2 Level 3) containing 488 tumor
122 and 58 non-tumor samples and Infinium Human Methylation 450K data (Level 3) containing
123 473 tumor and 32 non-tumorous samples of LADC cases with clinical annotations were
124 downloaded from The Cancer Genome Atlas (TCGA) Research Network
125 (<http://cancergenome.nih.gov>). mRNA expression data and DNA methylation data were
126 available for 36 and 29 paired tumorous/non-tumorous sample sets, respectively; both types of
127 data were available for 18 sets. Tumorous samples with mRNA expression data and survival

128 data were available for 423 cases. Survival analyses were conducted on patients with
129 normalized mRNA expression and overall survival (OS) profiles. Patients were divided into
130 low- and high-expression groups according to the median *GADI* mRNA expression value.

131 Kaplan-Meier Plotter (KM plotter, <http://kmplot.com/analysis/>), a publicly available online
132 database of published microarray datasets for primary tumors with clinical information [12],
133 was also used to generate OS curves in 9 studies from Gene Expression Omnibus (GEO,
134 <https://www.ncbi.nlm.nih.gov/geo/>, Supplementary Table S5) by setting the auto-selected best
135 value of *GADI* mRNA expression as the cutoff. All other parameters were left at default
136 settings.

137

138 *2.7. Immunohistochemical staining*

139 Paraffin sections (4 μ m thick) were subjected to immunohistochemical staining using the
140 Envision system (ChemMate Envision kit; Dako, Glostrup, Denmark) according to the
141 manufacturer's instructions. Antigen retrieval was performed by heating the dewaxed and
142 dehydrated sections in Dako Real Target Retrieval Solution, pH 9 (Dako), using a 2100 retriever
143 (Aptum Biologics, Ltd., Southampton, UK). A mouse anti-GAD67 monoclonal antibody
144 (Sigma-Aldrich, St. Louis, MO, USA; G5419), diluted to 1:200 with antibody diluents (Dako),
145 was used as the primary antibody. The proportion and intensity of GAD1 staining in the LADC
146 samples were scored (Supplementary Table S6A) independently by two different researchers.

147

148 *2.8. Statistical analysis*

149 Student's *t*-test or Fischer's exact test was used for comparisons between two groups. The
150 paired *t*-test was used for comparisons between paired samples. The relationship between
151 continuous variables was investigated by calculating the Spearman's correlation coefficient. For
152 survival analysis, Kaplan–Meier survival curves were constructed for groups based on
153 univariate predictors, and differences among groups were tested with the log-rank test.

154 Univariate and multivariate survival analyses were performed using the likelihood ratio test of
155 the stratified Cox proportional hazard regression analysis. Differences were assessed using two-
156 sided tests and were considered significant at a P -value of < 0.05 . Statistical analyses were
157 performed using IBM SPSS version 24 (IBM Corporation, Armonk, NY, USA) or the Survival
158 package for R (<https://cran.r-project.org>).

159

160 3. RESULTS

161 3.1. Methylation status of CGIs and each CpG site within CGIs around *GAD1*

162 In a previous array-based, genome-wide methylation screening of 12 paired tumorous/non-
163 tumorous LADC sample sets [4], CGI-3 around *GAD1* was ranked 14th as a hypermethylated
164 CGI with a high P -value (Supplementary Table S1). Because hypermethylation-associated
165 overexpression of *GAD1* was reported in colorectal and liver cancers [5], we re-evaluated the
166 results of the array-based methylation status of each CpG site within CGI-1–4 (Fig. 1A) around
167 *GAD1* (Fig. 1B). The methylation levels of all CpG sites determined by array-based analysis
168 within CGI-3 and in tumors were significantly higher than those in paired non-tumorous tissues.
169 Although the methylation levels in tumors were higher in CpG sites within CGI-3 than in those
170 within CGI-4, the average β -value in non-tumor tissues was extremely and specifically low at
171 cg15126544 and showed the largest difference of average β -value between tumors and non-
172 tumor tissues at this site (Fig. 1B and Supplementary Table S7), which is localized within the
173 CCCTC-binding factor (CTCF)-binding site of *GAD1*. Similar results were observed in the
174 Level 3 Infinium Human Methylation 450K data of 29 LADC tumors and paired non-tumor
175 tissues from TCGA dataset (Supplementary Fig. S1). Because hypermethylation around this
176 CTCF-binding site has been reported as a possible cause of *GAD1* overexpression [5], we
177 further assessed the methylation status of cg15126544 and *GAD1* mRNA expression levels.

178

179 3.2. Correlation between *GAD1* expression and CGI methylation in LADC clinical cases

180 The DNA methylation status and mRNA expression status were investigated in our panel of
181 LADC tumorous and paired non-tumorous tissues (Supplementary Table S2) using
182 pyrosequence-based methylation assays and rqRT-PCR-based expression analysis, respectively.
183 Of the 33 sample sets, 26 (78.8%) demonstrated significantly higher methylation levels in tumor
184 samples than in non-tumorous tissues (Fig. 1C). In the same cases, the mean *GADI* mRNA
185 expression levels in the tumors were significantly higher than those in the paired non-tumorous
186 tissues (Fig. 1D). There was a slightly positive ($\rho = 0.251$) but significant correlation between
187 methylation levels at cg15126544 and *GADI* mRNA expression (Fig. 1E). The LADC sample
188 set containing 18-paired samples obtained from TCGA demonstrated similar results both in
189 methylation levels at cg15126544 and *GADI* mRNA expression (Fig. 1F, 1G and
190 Supplementary Fig. S1). A significant and highly positive correlation between them was also
191 observed in TCGA dataset ($\rho = 0.706$, Fig. 1H). Because the gene expression status of cancer
192 cells directly affects their phenotypes, including malignant features, we focused on *GADI*
193 expression in tumors to further assess its prognostic significance in patients with LADC.

194

195 *3.3. Association of GADI mRNA expression levels with prognosis in LADC tumors*

196 In our LADC cohort, a sufficient number of cases with high-quality RNA suitable for
197 expression analysis was not available for survival analysis. Therefore, to test the association
198 between *GADI* mRNA expression levels in tumors and patients' prognosis, we first performed
199 survival analysis of 423 patients with LADC using data obtained from TCGA dataset. The OS
200 rate of patients with LADC with higher *GADI* mRNA expression in tumors was significantly
201 poorer than that of patients with lower *GADI* mRNA expression in tumors (Fig. 2A). Univariate
202 Cox regression analysis using data obtained from TCGA dataset confirmed that high *GADI*
203 mRNA expression was associated with a worse prognostic significance for OS (Table 1). In
204 multivariate Cox regression analysis, high *GADI* mRNA expression was also significantly

205 associated with a poorer OS rate, suggesting that *GAD1* mRNA expression is an independent
206 prognostic factor for OS ($P = 0.036$, Table 1).

207 To validate this result, we performed survival analysis by drawing Kaplan-Meier survival
208 curves using KM plotter (Fig. 2B). A total of 9 studies from the GEO dataset were included
209 (Supplementary Table S5). In a total of 720 patients with LADC from 9 cohorts, high *GAD1*
210 mRNA expression also significantly correlated with worse OS. In subgroup analysis of OS
211 using datasets of KM plotter, heterogeneous results were obtained among different cohorts.
212 Larger cohorts such as GSE31210 and GSE50081 consistently showed that higher *GAD1*
213 mRNA expression was a poor prognostic factor, whereas cohorts with a smaller number of cases
214 showed varying results (Supplementary Fig. S2). The results of univariate Cox regression
215 analysis confirmed these results (Fig. 2C).

216

217 *3.4. Immunohistochemical staining pattern of GAD1 and its association with prognosis in* 218 *LADC tumors*

219 To further validate the prognostic significance of GAD1 expression status, we further examined
220 the correlation between GAD1 protein expression and clinicopathological features including
221 prognosis in patients with LADC. We performed immunohistochemical staining of GAD1 in
222 tissue samples from our cohort of 162 patients with LADC (Supplementary Table S3).
223 Cytoplasmic GAD1 staining was observed in LADC tumor cells with higher mRNA expression,
224 whereas nearly no staining was observed in normal lung epithelial cells and either tumorous or
225 non-tumorous epithelial cells in LADC with lower mRNA expression (Fig. 3A). According to
226 the staining score (Supplementary Table S6B), 112 patients (69.1%) were classified into the
227 group with tumors showing GAD1 protein overexpression (positive GAD1 immunoreactivity).
228 Among the various clinicopathological factors, the pathological stage, pleural invasion, and
229 lymph vessel invasion were identified as factors significantly and positively associated with

230 positive GAD1 immunoreactivity (Table 2). Lymph node metastasis also tended to be more
231 frequently observed in the positive GAD1 immunoreactivity group.

232 According to the GAD1 protein expression status of LADC tumors, Kaplan-Meier curves
233 of estimated OS, disease-free survival (DFS), and cancer-specific survival (CSS) were
234 generated. Patients with GAD1 protein-overexpressing tumors showed significantly poorer DFS
235 ($P < 0.001$, log-rank test) and CSS ($P = 0.031$, log-rank test) than those without GAD1 protein
236 overexpressing tumors. Patients with GAD1 protein-overexpressing tumors tended to show
237 poorer OS, although the difference between groups was not significant (Fig. 3B). Univariate
238 Cox regression analysis confirmed that positive GAD1 immunoreactivity was significantly
239 associated with a worse prognostic significance for DFS (Table 3). Multivariate Cox regression
240 analysis in 162 patients revealed that GAD1 immunoreactivity was an independent prognostic
241 factor for DFS ($P = 0.011$, hazard ratio = 6.424, Table 3), but not for OS and CSS
242 (Supplementary Table S8 and S9).

243

244 4. DISCUSSION

245 In the present study, we focused on *GAD1* as a hypermethylated gene at specific CpG sites in
246 LADC tumors and demonstrated its overexpression in tumor-specific and methylation level-
247 associated manners in LADC. We also demonstrated the prognostic significance of GAD1
248 mRNA and protein expression levels in resected LADC tumors using various independent
249 publicly available datasets and our cohort, respectively. Our study suggested that GAD1
250 overexpression may be a useful biomarker for predicting the prognosis of patients with LADC.

251 GAD1 is known to catalyze the production of γ -aminobutyric acid (GABA) from L-
252 glutamic acid, the principal inhibitory neurotransmitter in the brain [13, 14]. GAD1
253 overexpression has been reported in various neoplastic tissues, but not in LADC. Moreover, the
254 associations between clinicopathological characteristics and GAD1 expression have not been
255 well-established. The most striking finding in this study is the prognostic significance of GAD1

256 mRNA and protein expression in patients with LADC. Although a sufficient number of RNA
257 samples suitable for expression analysis was not available in our cohort for survival analyses,
258 we used various publicly available data and demonstrated that *GAD1* mRNA overexpression in
259 tumors was significantly associated with poor prognosis (OS) in independent TCGA and GEO
260 datasets of LADC cases. In immunohistochemical analysis using our cohort, a positive
261 cytoplasmic *GAD1* staining pattern in tumor cells was significantly associated with poor
262 prognosis, particularly DFS but not OS, in patients with LADC. Although the difference in the
263 association between *GAD1* expression and OS among datasets remains unclear, it may be
264 explained by (1) variations in *GAD1* mRNA and protein expression, (2) the smaller size of the
265 cohort for immunohistochemical analysis compared to those of cohorts used for mRNA analysis
266 used in our study, and (3) variations in *GAD1* expression level and/or pattern among different
267 ethnicities.

268 Our study also demonstrated that *GAD1* protein expression in LADC was significantly
269 associated with pleural invasion and lymph vessel invasion. These findings suggest that *GAD1*
270 overexpression might be closely associated with cellular invasion. This hypothesis is supported
271 by previous reports of another cancers. Kimura et al. [6] demonstrated that *GAD1* promotes the
272 cancer cell invasion and metastasis of oral cancer by inducing the nuclear translocation of β -
273 catenin and secretion of MMP7 [15-20], although the regulatory mechanisms of *GAD1* in β -
274 catenin translocation remain unclear. In a brain metastasis model, it was reported that the
275 metastatic activity of tumor cells depends on the *GAD1*-GABA synthesis pathway [21]. Further
276 studies are needed to clarify the tumor-promoting activity of overexpressed *GAD1*.

277 Recently, Yan *et al.* [5] reported hypermethylation-associated *GAD1* overexpression in
278 colorectal and liver cancers and found that this paradoxical effect was caused by the
279 hypermethylation of the CTCF-binding site within *GAD1*, which may prevent CTCF binding,
280 inhibit CTCF-mediated repressive Polycomb repressive complex 2 (PRC2) complex recruitment
281 to the *GAD1* promoter, inhibit PRC2-induced trimethylation of histone H3 lysine 27

282 (H3K27m3), and eliminate the blocking activity H3K27m3 for *GAD1* transcription [22, 23].
283 These observations are contradictory to the well-established paradigm that promoter DNA
284 methylation represses transcription by inhibiting transcription factor binding and/or chromatin
285 structure modification [24-26]. In this study, we also detected hypermethylation at cg15126544
286 within the CTCF-binding site in LADC tumors, and tumor-specific *GAD1* overexpression was
287 positively associated with hypermethylation at cg15126544 in our cohort and the TCGA dataset.
288 Therefore, methylation of CTCF-binding sites may regulate *GAD1* expression in LADC as well.
289 However, it remains unknown whether the methylation of CGI or each CpG site around *GAD1*,
290 particularly cg15126544, is the only mechanism underlying the regulation of its transcription.
291 Interestingly, in brain metastatic tumor cells, it was reported that the downregulation of the
292 DNA methyltransferase DNMT1 induced by the brain microenvironment-derived clusterin
293 resulted in decreased *GAD1* promoter methylation and subsequent upregulation of *GAD1*
294 expression [21]. Therefore, even the effect of methylation levels of CpG sites around *GAD1* on
295 its expression level may vary under different conditions or in different cell lineages. Indeed,
296 MethSurv, a web tool for multivariable survival analysis using DNA methylation data obtained
297 from TCGA datasets (<https://biit.cs.ut.ee/methsurv/>), failed to show the prognostic significance
298 of CpG sites around *GAD1*, including cg15126544 for OS (data not shown). Therefore, the
299 methylation status of some CpG sites around *GAD1* may contribute to its gene expression at
300 some stages of LADC development, but not to the progression of this tumor. The *GAD1* mRNA
301 expression level data in normal lung tissues available in public databases, such as the NIH
302 Genotype-Tissue Expression Project (<https://www.gtexportal.org/>), as well as our
303 immunohistochemical staining results revealed no or low *GAD1* expression in normal lung
304 tissue, suggesting that *GAD1* is specifically expressed in tumor cells and contributes to the
305 progression of tumors in LADC. Because the gene expression status appears to more directly
306 contribute to the establishment of clinicopathological phenotypes in tumor cells, it is necessary

307 to investigate the detailed regulatory mechanisms of GAD1 expression in LADC cells at each
308 developmental stage of the tumor.

309 There are some limitations to this study. First, we demonstrated the prognostic impact of
310 GAD1 mRNA and protein statuses mainly in Caucasian and Japanese (Asian) populations,
311 respectively, but no data are available to directly compare GAD1 mRNA and protein expression
312 levels among different ethnicities. Because it has been reported that the frequency of acquired
313 alterations, such as epidermal growth factor receptor mutation, in lung tumors can vary across
314 different ethnicities [27-29], it is possible that the GAD1 expression pattern and/or levels differ
315 between Caucasian and Asian populations. However, the prognostic significance of the *GAD1*
316 mRNA expression status in Japanese cases with LADC was demonstrated by GSE31210 in
317 GEO datasets (Fig. 2C and Supplementary Fig. S2). Meta-analysis using 9 GEO datasets,
318 including GSE31210 and 8 other studies from western countries (Supplementary Table S5) also
319 revealed the prognostic significance of the GAD1 mRNA expression status (Fig. 2C),
320 suggesting that GAD1 overexpression is a common prognostic factor in various populations.
321 Second, our patient cohort was relatively small even for immunohistochemical analysis, and a
322 sufficient number of samples was not available for mRNA expression analysis to perform
323 survival analysis. Prospective multi-institutional studies are needed to further validate the
324 prognostic value of GAD1 overexpression in patients with LADC.

325

326 **5. CONCLUSION**

327 GAD1 overexpression appears to be a significant and independent prognostic indicator in
328 patients with resected LADC at both the mRNA and protein levels. This information may be
329 helpful for identifying patients at high risk of recurrence and overall survival after tumor
330 resection of LADC.

331

332 **REFERENCES**

333

334 1. Torre LA, Bray F, Siegel RL, et al. Global cancer statistics, 2012. *Cancer J Clin.*
335 2015;65(2):87–108.

336

337 2. Travis WD, Brambilla E, Noguchi M, et al. International Association for the Study of Lung
338 Cancer/American Thoracic Society/European Respiratory Society international
339 multidisciplinary classification of lung adenocarcinoma. *J Thorac Oncol.* 2011;6(2):244–285.

340

341 3. Johnson DH, Schiller JH. Recent clinical advances in lung cancer management. *J Clin Oncol.*
342 2014;32(10):973–982.

343

344 4. Kajiura K, Masuda K, Naruto T, et al. Frequent silencing of the candidate tumor suppressor
345 TRIM58 by promoter methylation in early-stage lung adenocarcinoma. *Oncotarget.*
346 2017;10(2):2890–2905.

347

348 5. Yan H, Tang G, Wang H, et al. DNA methylation reactivates GAD1 expression in cancer by
349 preventing CTCF-mediated polycomb repressive complex 2 recruitment. *Oncogene.*
350 2016;35(30):3995–4008.

351

352 6. Kimura R, Kasamatsu A, Koyama T, et al. Glutamate acid decarboxylase 1 promotes
353 metastasis of human oral cancer by beta-catenin translocation and MMP7 activation. *BMC*
354 *Cancer.* 2013;13:555.

355

356 7. Lee YY, Chao TB, Sheu MJ, et al. Glutamate decarboxylase 1 overexpression as a poor
357 prognostic factor in patients with nasopharyngeal carcinoma. *J Cancer.* 2016;7(12):1716–1723.

358

359 8. Maemura K, Yamauchi H, Hayasaki H, et al. Gamma-amino-butyric acid immunoreactivity in
360 intramucosal colonic tumors. *J Gastroenterol Hepatol*. 2003;18(9):1089–1094.

361

362 9. Matuszek M, Jesipowicz M, Kleinrok Z. GABA content and GAD activity in gastric cancer.
363 *Med Sci Monit*. 2001;7(3):377-381.

364

365 10. Goldstraw P, Crowley J, Chansky K, et al. International Association for the Study of Lung
366 Cancer International Staging Committee, and Participating Institutions. The IASLC Lung
367 Cancer Staging Project: proposals for the revision of the TNM stage groupings in the
368 forthcoming (seventh) edition of the TNM Classification of malignant tumours. *J Thorac Oncol*
369 2007;2(8):706–714.

370

371 11. Travis WD, Brambilla E, Burke AP, Marx A, Nicholson, AG. WHO classification of tumours
372 of the lung, pleura, thymus and heart. Fourth edition. Lyon: International Agency for Research
373 on Cancer; 2015.

374

375 12. Györfly B, Surowiak P, Budzies J, Lániczky A. Online survival analysis software to assess
376 the prognostic value of biomarkers using transcriptomic data in non-small-cell lung cancer.
377 *PLoS One*. 2013;18:e82241.

378

379 13. Erlander MG, Tobin AJ. The structural and functional heterogeneity of glutamic acid
380 decarboxylase: a review. *Neurochem Res*. 1991;16(3):215–226.

381

382 14. Young SZ, Bordey A. GABA's control of stem and cancer cell proliferation in
383 adult neural and peripheral niches. *Physiology (Bethesda)*. 2009;24:171–185.

384

385 15. Kruck S, Eyrich C, Scharpf M, et al. Impact of an altered Wnt1/ β -catenin expression on
386 clinicopathology and prognosis in clear cell renal cell carcinoma. *Int J Mol Sci*.
387 2013;14(6):10944–10957.

388

389 16. Sawada G, Ueo H, Matsumura T, et al. CHD8 is an independent prognostic indicator that
390 regulates Wnt/ β -catenin signaling and the cell cycle in gastric cancer. *Oncol Rep*.
391 2013;30(3):1137–1142.

392

393 17. Abd El-Rehim D, Ali MM. Aberrant expression of β -catenin in invasive ductal breast
394 carcinomas. *J Egypt Natl Canc Inst*. 2009;21(2):185–195.

395

396 18. Ishikawa T, Kimura Y, Hirano H, Higashi S. Matrix metalloproteinase-7 induces homotypic
397 tumor cell aggregation via proteolytic cleavage of the membrane-bound Kunitz-type inhibitor
398 HAI-1. *J Biol Chem*. 2017;292(50):20769–20784.

399

400 19. Mylona E, Kapranou A, Mavrommatis J, et al. The multifunctional role of the
401 immunohistochemical expression of MMP-7 in invasive breast cancer. *APMIS*.
402 2005;113(4):246–255.

403

404 20. Wang FQ, So J, Reierstad S, Fishman DA. Matrilysin (MMP-7) promotes invasion of ovarian
405 cancer cells by activation of progelatinase. *Int J Cancer*. 2005;114(1):19–31.

406

407 21. Schnepf PM, Lee DD, Guldner IH, et al. GAD1 upregulation programs aggressive features
408 of cancer cell metabolism in the brain metastatic microenvironment. *Cancer Res*.
409 2017;77(11):2844–2856.

410

411 22. Schuettengruber B, Chourrout D, Vervoort M, et al. Genome regulation by polycomb and
412 trithorax proteins. *Cell*. 2007;128(4):735–745.

413

414 23. Li T, Hu JF, Qiu X, et al. CTCF regulates allelic expression of *Igf2* by orchestrating a
415 promoter-polycomb repressive complex 2 intrachromosomal loop. *Mol Cell Biol*.
416 2008;28(20):6473–6482.

417

418 24. Razin A, Riggs AD. DNA methylation and gene function. *Science*. 1980;210(4470):604–
419 610.

420

421 25. Holliday R, Pugh JE. DNA modification mechanisms and gene activity during development.
422 *Science*. 1975;187(4173):226–232.

423

424 26. Bird A. Perceptions of epigenetics. *Nature*. 2007;447(7143):396–398.

425

426 27. Arrieta O, Cardona AF, Martín C, et al. Updated frequency of EGFR and KRAS mutations
427 in non-small-cell lung cancer in Latin America: The Latin-American consortium for the
428 investigation of lung cancer (CLICaP). *J Thorac Oncol*. 2015;10(5):838–843.

429

430 28. Shigematsu H, Lin L, Takahashi T, et al. Clinical and biological features associated with
431 epidermal growth factor receptor gene mutations in lung cancers. *J Natl Cancer Inst*.
432 2005;97(5):339–346.

433

434 29. Campbell JD, Lathan C, Sholl L, et al. Comparison of Prevalence and Types of Mutations in
435 Lung Cancers Among Black and White Populations. *JAMA Oncol*. 2017;3(6):801–809.

436
437

Table 1. Cox proportional hazard regression analysis of overall survival in 400 patients with LADC in TCGA dataset

Factor (number)	Univariate			Multivariate		
	Hazard ratio	95% confidence interval	P-value	Hazard ratio	95% confidence interval	P-value
Sex						
Male (n = 184) vs. Female (n = 216)	1.048	0.704 – 1.560	0.818	1.087	0.705 – 1.675	0.706
Age (years)						
>67 (n = 210) vs. ≤67 (n = 190)	1.348	0.897 – 2.025	0.151	1.639	1.079 – 2.490	0.021
Smoking history						
Positive (n = 339) vs. Negative (n = 61)	1.069	0.569 – 2.006	0.836	1.521	0.766 – 3.020	0.230
Pathological stage						
II, III, IV (n = 184) vs. I (n=216)	2.620	1.725 – 3.979	6.21E-6	-	-	-
Tumor size						
pT2-4 (n = 272) vs. pT1 (n = 128)	1.631	0.978 – 2.720	0.0609	1.565	0.922 – 2.658	0.097
N stage (pN)						
pN1-3 (n = 136) vs. pN0 (n = 264)	2.475	1.662 – 3.688	8.32E-6	2.487	1.649 – 3.750	1.38E-5
M stage (pM)						
pM1 (n 19) vs. pM0 (n = 381)	1.539	0.773 - 3.066	0.220	1.528	0.752 – 3.103	0.241
<i>GAD1</i> mRNA expression						
High (n = 217) vs. Low (n = 183)	1.749	1.165 – 2.626	6.97E-3	1.573	1.029 – 2.404	0.036

438
439
440
441

Statistically significant values are in boldface type.

The analysis was performed in 400 patients with complete clinical information in the TCGA dataset.

The population was divided using the auto-selected best value of *GAD1* mRNA expression as the cutoff.

442
443

Table 2. Correlation between GAD1 immunoreactivity and clinicopathological factors in 162 patients with LADC

Factor	GAD1 immunoreactivity (n = 162)		P-value ^a
	Negative (n = 50)	Positive (n = 112)	
Male / Female	26 / 24	55 / 57	0.865
Age ^b	69.0 ± 9.6	67.4 ± 9.0	0.386
Smoking history ^{b, c} (+/-)	22 / 27	55 / 56	0.603
Brinkman index ^{b, c}	406.5 ± 536.4	485.0 ± 622.7	0.461
Tumor size ^{b, c}	23.5 ± 14.3	26.1 ± 13.4	0.226
pStage (I/II+III)	39 / 11	65 / 47	0.021
Lymph node metastasis (+/-)	8 / 42	36 / 76	0.054
Pleural invasion ^c (+/-)	5 / 40	35 / 72	0.005
Vascular invasion ^c (+/-)	5 / 40	22 / 79	0.284
Lymph vessel invasion ^c (+/-)	6 / 39	31 / 66	0.023
<i>EGFR</i> mutation ^c (+/-)	10 / 6	30 / 29	0.573
Predominant histologic subtype (lepidic / papillary / acinar/ solid/ enteric)	23 / 18 / 4 / 4 / 1	36 / 47 / 24 / 5 / 0	0.068

444
445
446
447
448
449

^aP-values were calculated using Fischer's exact test for gender, smoking history, lymph node metastasis, pleural invasion, lymph vessel invasion, and vascular invasion, *EGFR* mutation, and using Student's *t*-test for age, Brinkman index, and tumor size and using χ^2 test for trend for predominant histologic subtype. Statistically significant values ($P < 0.05$) are in boldface type.

^bAge, Brinkman index, and tumor size are expressed as the mean ± standard deviation.

^cData of these factors were not available for all patients.

450
451

Table 3. Cox proportional hazard regression analysis for disease-free survival in 162 patients with LADC

Factor	Univariate			Multivariate		
	Hazard ratio	95% confidence interval	P-value	Hazard ratio	95% confidence interval	P-value
Sex						
Male (n=81) vs. Female (n=81)	1.202	0.666 - 2.170	0.541	2.459	0.520 - 11.624	0.256
Age (years)						
>67 (n=87) vs. ≤67 (n=75)	1.048	0.582 - 1.887	0.875	0.995	0.515 - 1.922	0.988
Smoking history ^a						
Positive (n=77) vs. Negative (n=83)	1.302	0.724 - 2.344	0.378	0.324	0.068 - 1.546	0.158
Pathological stage						
II, III (n=58) vs. I (n=104)	7.466	3.769 - 14.789	< 0.001	-	-	-
Tumor size ^a						
pT2-4 (n=39) vs. pT1 (n=115)	2.309	1.241 - 4.296	0.008	2.033	0.961 - 4.303	0.070
N stage (pN)						
pN1-3 (n=44) vs. pN0 (n=118)	7.100	3.837 - 13.140	< 0.001	2.507	1.057 - 5.949	0.037
Pleural invasion ^a						
Positive (n=40) vs. Negative (n=112)	4.926	2.637 - 9.202	< 0.001	2.091	0.977 - 4.478	0.058
Vascular invasion ^a						
Positive (n=27) vs. Negative (n=119)	4.706	2.529 - 8.757	< 0.001	1.139	0.389 - 3.341	0.812
Lymph vessel invasion ^a						
Positive (n=37) vs. Negative (n=105)	5.346	2.809 - 10.175	< 0.001	1.355	0.478 - 3.847	0.568
Adjuvant chemotherapy ^a						
With (n=47) vs. Without (n=106)	2.972	1.614 - 5.470	< 0.001	-	-	-
EGFR mutation ^a						
Negative (n=35) vs. Positive (n=40)	1.285	0.678 - 2.433	0.442	-	-	-
Predominant subtype						
Non-lepidic (n=103) vs. Lepidic (n=59)	6.711	2.392 - 18.868	< 0.001	2.725	0.861 - 8.621	0.088
GAD1 immunoreactivity						
Positive (n=112) vs. Negative (n=50)	9.341	2.248 - 38.824	0.002	6.424	1.522 - 27.108	0.011

452

Statistically significant values are in boldface type.

453

^aData of these factors were not available for all patients.

454

455
456

Supplementary Table S1. The top 14 CpG islands significantly hypermethylated in tumorous tissues of 12 stage-I LADC cases⁴

No.	CpG island	Adjusted <i>P</i> -value ^a	β -difference ^b	Gene name
1	chr7:153583317-153585666	0.000495704	0.277562652	<i>DPP6</i>
2	chr19:52390841-52391368	0.000671077	0.291495741	<i>ZNF577</i>
3	chr11:125774292-125774584	0.000839411	0.271871389	<i>DDX25</i>
4	chr3:62355315-62355534	0.001348289	0.25890625	<i>FEZF2</i>
5	chr1:156863415-156863711	0.001564128	0.369176667	<i>PEAR1</i>
6	chr15:37390175-37390380	0.002225792	0.324917222	<i>MEIS2</i>
7	chr1:248020330-248021252	0.00443318	0.270335	<i>TRIM58</i>
8	chr12:103696090-103696418	0.006552561	0.318931667	<i>C12orf42</i>
9	chr7:158110569-158110881	0.008975336	0.270233333	<i>PTPRN2</i>
10	chr6:50810642-50810994	0.010799023	0.30752125	<i>TFAP2B</i>
11	chr5:134363092-134365146	0.011483039	0.262798796	<i>PITX1</i>
12	chr19:58545115-58545897	0.011599292	0.27722213	<i>ZSCAN1</i>
13	chr6:50791110-50791573	0.012733507	0.331794167	<i>TFAP2B</i>
14	chr2:171676552-171676980	0.017464759	0.251871944	<i>GADI</i>

457

The row corresponding to *GADI* is in boldface type.

458

^aDifferences between methylation levels (β -values) of CpG islands in tumors and paired non-tumorous tissues were assessed by paired *t*-test. *P*-values were adjusted with the Benjamini–Hochberg correction (false discovery rate, FDR). CpG islands were sorted by the adjusted *P*-value.

459

460

461

^b β -differences (differential methylation levels) represent the average of [(β -value of tumorous tissue) - (β -value of paired non-tumorous tissue)] in 12 stage-I LADC cases.

462

463

464 Supplementary Table S2. Clinicopathological characteristics of 33 patients with LADC analyzed by qPCR and pyrosequencing
465

Characteristics	Number
Gender	
Male	18
Female	15
Age (years)	62.9 ± 9.6
Stage	
Ia, Ib	16
IIa, IIb	8
IIIa, IIIb	9
Smoking History	
+	15
-	18
Brinkman Index	616.7 ± 745.4

466 Age and Brinkman index are expressed as the mean ± standard deviation.

467
468

469
470

Supplementary Table S3. Characteristics of 162 patients with LADC analyzed by immunohistochemistry

Characteristics	N = 162 (%)
Gender	
Male	81 (50.0%)
Female	81 (50.0%)
Age (years)	67.0 ± 9.2
Stage	
Ia, Ib	104 (64.2%)
IIa, IIb	26 (16.0%)
IIIa, IIIb	32 (19.8%)
<i>EGFR</i> mutation	
Positive	40 (24.7%)
Negative	35 (21.6%)
Unknown	87 (53.7%)
Predominant histologic subtype	
lepidic	59 (36.4%)
papillary	65 (40.1%)
acinar	28 (17.3%)
solid	9 (5.6%)
enteric	1 (0.6%)
Adjuvant chemotherapy	
With	47 (29.0%)
Without	106 (65.4%)
Unknown	9 (5.6%)
Smoking History	
+	78 (48.1%)
-	82 (50.6%)
Unknown	2 (1.2%)
Brinkman Index	461.0 ± 597.0

471

Age and Brinkman index are expressed as the mean ± standard deviation.

472 Supplementary Table S4. List of primer sets used in qPCR and pyrosequencing
 473

Gene/primer name		Sequence/ID
TaqMan gene expression assay		
<i>GAD1</i>	FAM	Hs01065893_m1
<i>GAPDH</i>	FAM	Hs02758991_g1
Pyrosequencing of <i>GAD1</i>		
cg15126544	Forward	5'-TGGTTTTTAGGGTTTTTTTTTTTGA-3'
	Reverse	5'-ACAAATACACCCCTTAATCTACTCTCC-3'
	Sequence	5'-GTAGAAGAGGGAGGAA-3'

474
 475
 476

477
478

Supplementary Table S5. List of GEO data sets

GEO accession	Survival period	Submission date	Number of patients	Country	Race	Platform
GSE14814	from date of random assignment to death from disease or treatment complication	12-Feb-9	27	Canada USA Germany	NA	HG-U133A,
GSE19188	NA	25-Nov-9	41	Netherlands	Mostly Caucasian	HG-U133_Plus_2
GSE3141	NA	16-Aug-5	58	USA	NA	HG-U133_Plus_2
GSE50081	NA	21-Aug-13	127	Canada	NA	HG-U133_Plus_2
GSE31908	NA	6-Sep-11	20	USA	Mostly Caucasian	HG-U133A HG- U133B HG- U133_Plus_2
GSE37745	NA	3-May-12	106	Sweden	NA	HG-U133_Plus_2
GSE29013	from the date of surgery to death or the last follow-up contact.	2-May-11	30	USA	Mostly Caucasian	HG-U133_Plus_2
GSE30219	NA	26-Jun-11	85	France USA	NA	HG-U133_Plus_2
GSE31210	NA	4-Aug-11	226	Japan	Asian	HG-U133_Plus_2

479
480

481 Supplementary Table S6. Evaluation criteria for GAD1 immunohistochemistry

482

483 A. Proportion and intensity scores for GAD1 staining in immunohistochemical analysis

Proportion score (PS)		Intensity score (IS)	
Score	Observation	Score	Observation
1	< 25%	0	None
2	26 - 50%	1	Weak
3	51 - 75%	2	Intermediate
4	76% ≤	3	Strong

484

485 B. Evaluation of GAD1 immunoreactivity using PS and IS

GAD1 immunoreactivity	Sum of PS and IS	Number of cases
	1	0
Negative	2	14
	3	10
	4	26
	5	44
Positive	6	43
	7	25

486 The staining score is defined as the sum of the proportion and intensity scores.

487 A staining score ≥ 5 indicated overexpression of the GAD1 protein (positive GAD1 immunoreactivity).

488

489
490

Supplementary Table S7. The methylation levels of each CpG site of *GAD1* in tumorous and non-tumorous samples

CpG site	β-value (average ^a)		β-value (SD ^b)		P-value ^c	β-difference ^d
	Tumor	Non-tumor	Tumor	Non-tumor		
cg09404592	0.109475	0.0853917	0.04619235	0.02516931	0.1810443145	0.024083333
cg03443455	0.462661667	0.3074692	0.09759064	0.04014665	0.0004807189	0.1551925
cg00782607	0.106084167	0.0710583	0.04960498	0.03644913	0.0389929681	0.035025833
cg13612847	0.133873333	0.1472975	0.03817365	0.03253079	0.0972520412	-0.013424167
cg03448612	0.083106667	0.0758158	0.02049695	0.03057835	0.3611596712	0.007290833
cg09742688	0.019295	0.014535	0.00964859	0.00580472	0.1767899083	0.00476
cg23221504	0.100365	0.1095158	0.02678416	0.03834864	0.3202119878	-0.009150833
cg00915206	0.067003333	0.0671983	0.01743706	0.03309326	0.9850457390	-0.000195
cg11582100	0.05327	0.0542092	0.01019424	0.02677933	0.8871008599	-0.000939167
cg15306595	0.0394325	0.0438158	0.01045799	0.01931569	0.4524979803	-0.004383333
cg19538089	0.104192727	0.0801767	0.05266865	0.02819045	0.1330389745	0.024016061
cg26391350	0.086990833	0.0757083	0.02871752	0.03569546	0.2703867579	0.0112825
cg16911423	0.179124167	0.13477	0.05271661	0.02415412	0.0169907853	0.044354167
cg01763173	0.085408333	0.0639708	0.03334425	0.02293707	0.0705795610	0.0214375
cg11281641	0.154460833	0.0533167	0.0959479	0.02516992	0.0046353604	0.101144167
cg07420274	0.536216667	0.3580283	0.06408349	0.05326207	0.0001252001	0.178188333
cg01089249	0.529403333	0.2895042	0.06934644	0.02343744	0.0000006700	0.239899167
cg01089319	0.505844167	0.256055	0.06506377	0.03497551	0.0000011299	0.249789167
cg14005211	0.539773333	0.2738458	0.0827698	0.05432622	0.0000013853	0.2659275
cg14486905	0.46974	0.2449983	0.12168293	0.04163571	0.0002223438	0.224741667
cg09144707	0.494621667	0.2901625	0.10770392	0.03041366	0.0000452368	0.204459167
cg02723395	0.411985	0.1740225	0.15358608	0.0351129	0.0005880955	0.2379625
cg15126544	0.363693333	0.0397042	0.14160994	0.02161663	0.0000079194	0.323989167
cg04105250	0.337811667	0.1510408	0.11281548	0.02977583	0.0001733147	0.186770833
cg00729049	0.2934125	0.1690383	0.08912118	0.02842007	0.0014668716	0.124374167
cg15753746	0.363454167	0.1337517	0.17759626	0.03602908	0.0009859990	0.2297025
cg21535772	0.4300025	0.2728233	0.09775366	0.03462184	0.0004699895	0.157179167
cg19846314	0.445076667	0.2232308	0.17797695	0.07571523	0.0024014465	0.221845833
cg08863440	0.403660833	0.2232942	0.15063177	0.06307915	0.0033596932	0.180366667
cg07620853	0.5666125	0.5479283	0.19697479	0.14942316	0.7081756486	0.018684167

491
492
493
494
495
496
497
498
499

The row corresponding to cg15126544 is in **boldface type**.

^aThe average methylation level of 12 LADC samples.

^bThe standard deviation (SD) of methylation levels of 12 LADC samples.

^cDifferences between methylation levels (β-values) of CpG islands in tumors and paired non-tumorous tissues were assessed by paired *t*-test.

^dβ-differences (differential methylation levels) represent the average of [(β-value of tumorous tissue) - (β-value of paired non-tumorous tissue)] in 12 stage-I LADC cases.

500
501

Supplementary Table S8. Cox proportional hazard regression analysis of overall survival in 162 patients with LADC

Factor	Univariate			Multivariate		
	Hazard ratio	95% confidence interval	P-value	Hazard ratio	95% confidence interval	P-value
Sex						
Male (n=81) vs. Female (n=81)	3.219	1.452 - 7.138	0.004	1.311	0.220 - 7.802	1.311
Age (years)						
>67 (n=87) vs. ≤67 (n=75)	2.471	1.169 - 5.224	0.018	2.562	1.073 - 6.120	0.034
Smoking history ^a						
Positive (n=77) vs. Negative (n=83)	4.177	1.817 - 9.602	0.001	2.166	0.341 - 13.759	0.413
Pathological stage						
II, III (n=58) vs. I (n=104)	4.328	1.999 - 9.372	< 0.001	-	-	-
Tumor size ^a						
pT2-4 (n=39) vs. pT1 (n=115)	2.262	1.119 - 4.573	0.023	2.466	1.116 - 5.447	0.026
N stage (pN)						
pN1-3 (n=44) vs. pN0 (n=118)	3.577	1.789 - 7.151	< 0.001	0.909	0.343 - 2.410	0.848
Pleural invasion ^a						
Positive (n=40) vs. Negative (n=112)	2.051	0.987 - 4.264	0.054	1.635	0.626 - 4.267	0.315
Vascular invasion ^a						
Positive (n=27) vs. Negative (n=119)	2.735	1.284 - 5.826	0.009	0.487	0.157 - 1.512	0.213
Lymph vessel invasion ^a						
Positive (n=37) vs. Negative (n=105)	4.700	2.203 - 10.027	< 0.001	3.897	1.311 - 11.580	0.014
Adjuvant chemotherapy ^a						
With (n=47) vs. Without (n=106)	0.996	0.472 - 2.101	0.991	-	-	-
EGFR mutation ^a						
Negative (n=35) vs. Positive (n=40)	2.882	1.151 - 2.564	0.024	-	-	-
Predominant subtype						
Non-lepidic (n=103) vs. Lepidic (n=59)	3.311	1.156 - 9.524	0.026	2.841	0.590 - 13.699	0.193
GAD1 immunoreactivity						
Positive (n=112) vs. Negative (n=50)	2.315	0.895 - 5.992	0.084	1.216	0.366 - 4.042	0.750

502

Statistically significant values are in boldface type.

503

^aData of these factors were not available for all patients.

504

505
506

Supplementary Table S9. Cox proportional hazard regression analysis of cancer-specific survival in 162 patients with LADC

Factor	Univariate			Multivariate		
	Hazard ratio	95% confidence interval	P-value	Hazard ratio	95% confidence interval	P-value
Sex						
Male (n=81) vs. Female (n=81)	1.945	0.827 - 4.576	0.127	1.160	0.194 - 6.923	0.871
Age (years)						
>67 (n=87) vs. ≤67 (n=75)	1.735	0.749 - 4.021	0.199	1.932	0.748 - 4.987	0.173
Smoking history ^a						
Positive (n=77) vs. Negative (n=83)	2.599	1.076 - 6.279	0.034	1.398	0.221 - 8.839	0.722
Pathological stage						
II, III (n=58) vs. I (n=104)	7.706	2.606 - 22.791	< 0.001	-	-	-
Tumor size ^a						
pT2-4 (n=39) vs. pT1 (n=115)	1.994	0.847 - 4.697	0.114	1.867	0.733 - 4.758	0.191
N stage (pN)						
pN1-3 (n=44) vs. pN0 (n=118)	6.066	2.488 - 14.789	< 0.001	1.322	0.398 - 4.395	0.649
Pleural invasion ^a						
Positive (n=40) vs. Negative (n=112)	2.331	0.957 - 5.677	0.063	1.255	0.429 - 3.673	0.679
Vascular invasion ^a						
Positive (n=27) vs. Negative (n=119)	4.089	1.697 - 9.854	0.002	0.892	0.236 - 3.378	0.867
Lymph vessel invasion ^a						
Positive (n=37) vs. Negative (n=105)	5.610	2.239 - 14.055	< 0.001	2.654	0.703 - 10.022	0.150
Adjuvant chemotherapy ^a						
With (n=47) vs. Without (n=106)	1.036	0.428 - 2.504	0.938	-	-	-
EGFR mutation ^a						
Negative (n=35) vs. Positive (n=40)	3.165	1.188 - 8.403	0.021	-	-	-
Predominant subtype						
Non-lepidic (n=103) vs. Lepidic (n=59)	9.804	1.311 - 71.429	0.026	3.378	0.392 - 29.411	0.268
GAD1 immunoreactivity						
Positive (n=112) vs. Negative (n=50)	4.323	1.015 - 18.420	0.048	3.400	0.415 - 27.827	0.254

507

Statistically significant values are in boldface type.

508

^aData of these factors were not available for all patients.

509

510

511 **Figure Legends**

512

513 **Figure 1.** DNA methylation and mRNA expression status of *GADI* in patients with
514 LADC.

515 (A) A schematic diagram of the *GADI* gene structure with CGIs around *GADI*. The
516 arrow indicates the location of cg15126544.

517 (B) The average β -value (methylation level) of each CpG site targeted in the array-based
518 methylation experiment involving 12 LADC cases. * $P < 0.05$ vs. paired non-tumorous
519 tissues.

520 (C) Linear plots of the average DNA methylation values (percentages) of cg15126544 in
521 33 LADC tumorous and paired non-tumorous tissues, as determined by quantitative
522 pyrosequencing. Samples from the same patient are linked with straight lines.

523 (D) Linear plots of expression levels of *GADI* mRNA relative to those of the control
524 normal human lung in 33 LADC tumorous and paired non-tumorous tissues. Relative
525 expression of *GADI* mRNA was calculated using Human Lung Total RNA as a normal
526 control.

527 (E) Correlation between the average methylation levels of cg15126544 (x-axis) and
528 relative *GADI* mRNA expression levels (y-axis) in 33 LADC tumorous and paired non-
529 tumorous tissues.

530 (F) Linear plots of the methylation levels (β -values) of cg15126544 determined through
531 an array-based methylation experiment using HumanMethylation450K array in 18
532 paired LADC tumor and non-tumorous tissue samples obtained from the TCGA dataset
533 (<http://cancergenome.nih.gov>).

534 (G) Linear plots of mRNA expression of *GADI* determined by RNA sequencing and
535 quantified by RNA-Seq by Expectation Maximization (RSEM) in 18 paired LADC
536 tumor and non-tumorous tissue samples obtained from the TCGA dataset.

537 (H) Correlation between the methylation levels (β -values) of cg15126544 (x-axis) and
538 *GADI* mRNA expression levels (y-axis) in 18 paired LADC tumor and non-tumorous
539 tissue samples obtained from the TCGA dataset.

540

541 **Figure 2.** Publicly available datasets showing association between *GADI* mRNA
542 expression status and prognosis in patients with LADC.

543 (A) Kaplan-Meier curve for OS rate of 423 LADC patients according to *GADI* mRNA
544 expression levels using data obtained from the TCGA dataset. *P*-values were calculated
545 using the log-rank test. Statistically significant *P*-values are in boldface type.

546 (B) Kaplan-Meier curve for OS rate of 720 LADC patients in cohorts GSE14814,
547 GSE19188, GSE3141, GSE50081, GSE31908, GSE37745, GSE29013, GSE30219, and
548 GSE31210 according to *GADI* mRNA expression levels obtained from the online
549 survival analysis software, Kaplan–Meier plotter (KM plotter; <http://www.kmplot.com>).
550 *P*-values were calculated using the log-rank test. Statistically significant *P*-values are in
551 boldface type.

552 (C) Subgroup analysis of KM plotter databases for *GADI* mRNA expression in LADC.
553 Hazard ratios (HR, center of the box) and 95% confidence intervals (CI, horizontal line)
554 were calculated with Cox's regression models.

555

556 **Figure 3.** Association between *GAD1* protein expression status and prognosis in
557 patients with LADC.

558 (A) Representative images of immunohistochemically detected GAD1 protein in tumors
559 and non-tumorous lesions of LADC samples and normal lung tissue. Scale bars, 200
560 μm . The relative GAD1 mRNA expression level of each sample as determined by rqRT-
561 PCR is also shown.

562 (B) Kaplan-Meier curves for overall survival, disease-free survival, and cancer-specific
563 survival rates of 162 LADC patients according to the immunoreactivity of GAD1. *P*-
564 values were calculated using the log-rank test. Statistically significant *P*-values are in
565 boldface type.

566

567 **Supplementary Figure Legends**

568

569 **Supplementary Figure S1.** The average β -value (methylation level) of each CpG site
570 targeted in the Infinium HumanMethylation450K data (Level 3) of 29 paired LADC
571 tumor and non-tumorous tissue samples downloaded from TCGA Research Network
572 (<http://cancergenome.nih.gov>). Data of some CpG sites were missing in the TCGA
573 dataset. * $P < 0.05$ vs. paired non-tumorous tissues.

574

575 **Supplementary Figure S2.** Kaplan-Meier overall survival curves of all selected
576 datasets from KM plotter used in the present study (see Figure 2C). Hazard ratios (HR)
577 and 95% confidence intervals in parentheses are shown for each dataset. P -values were
578 calculated using the log-rank test.

579

580

581 **ACKNOWLEDGMENT**

582 The authors would like to thank Dr. Yoshimi Bando, Division of Pathology, Tokushima
583 University Hospital for her contributing to this study. This work was supported by JSPS
584 KAKENHI (grant number JP18H02894). The funding source was not involved in the
585 design of the study, in the collection, analysis, and interpretation of results, in the
586 preparation of the manuscript, or in the decision to submit the article for publication.

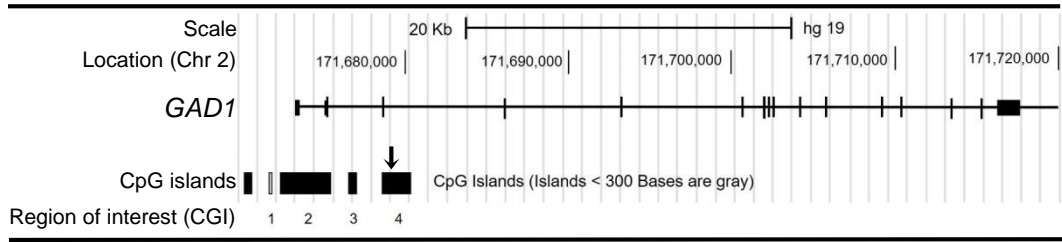
587

588 **CONFLICT OF INTEREST**

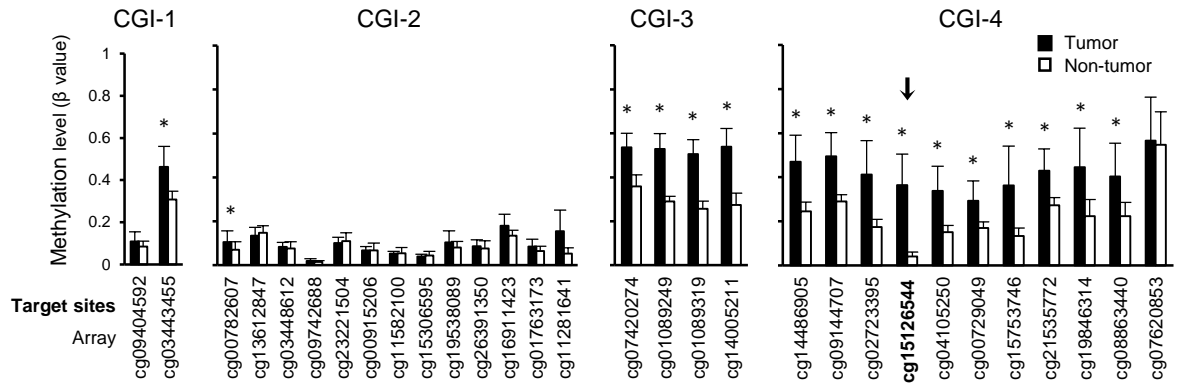
589 All authors declare no conflicts of interest associated with this manuscript.

Figure 1

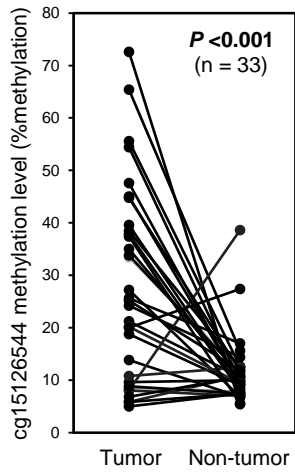
A



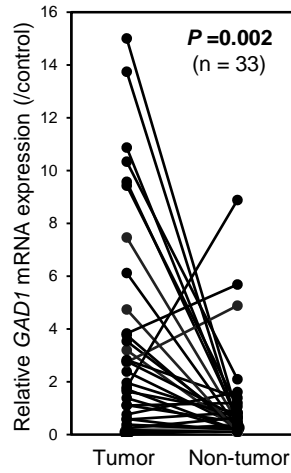
B



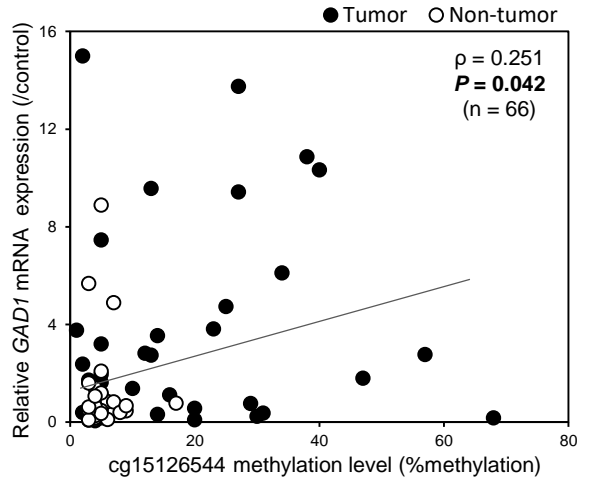
C



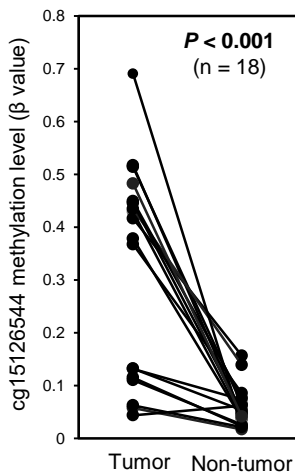
D



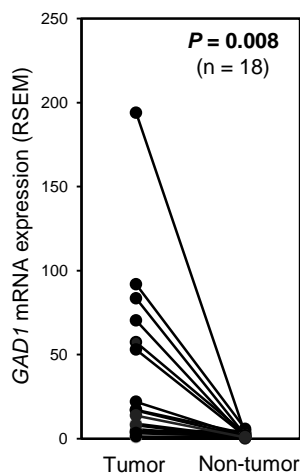
E



F



G



H

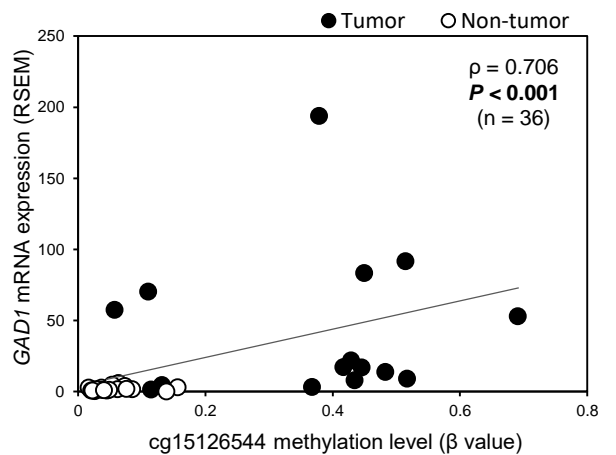


Figure 2

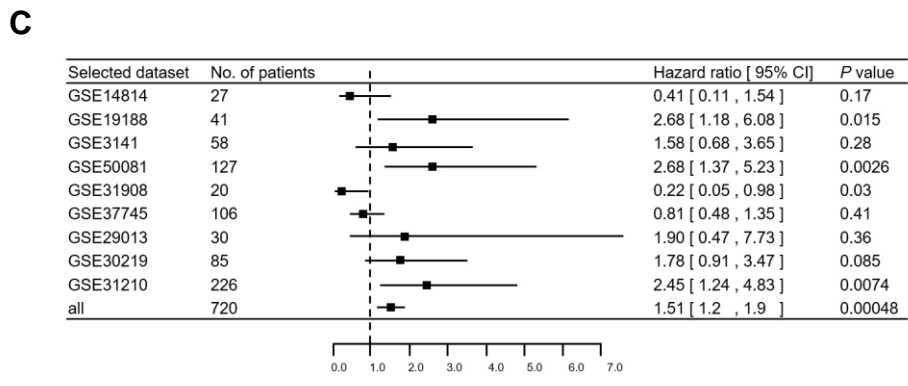
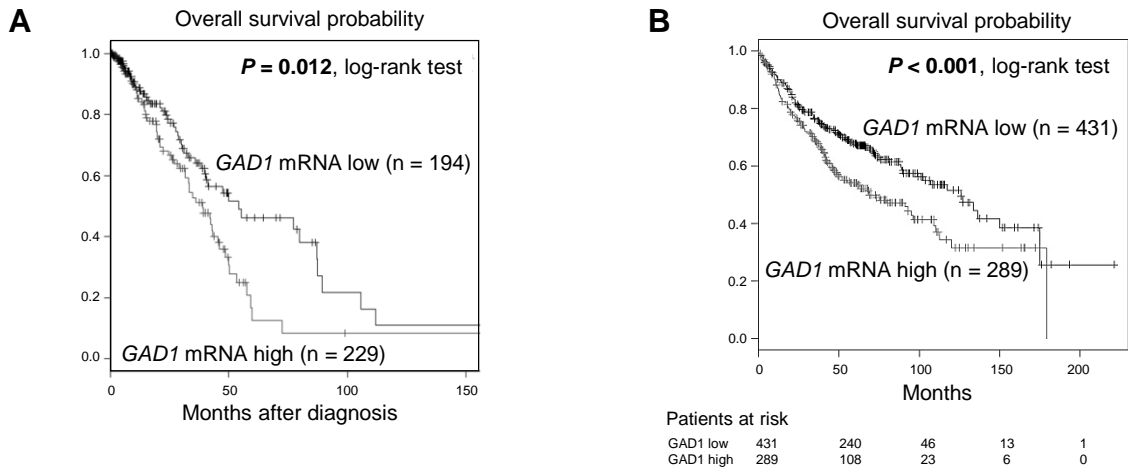
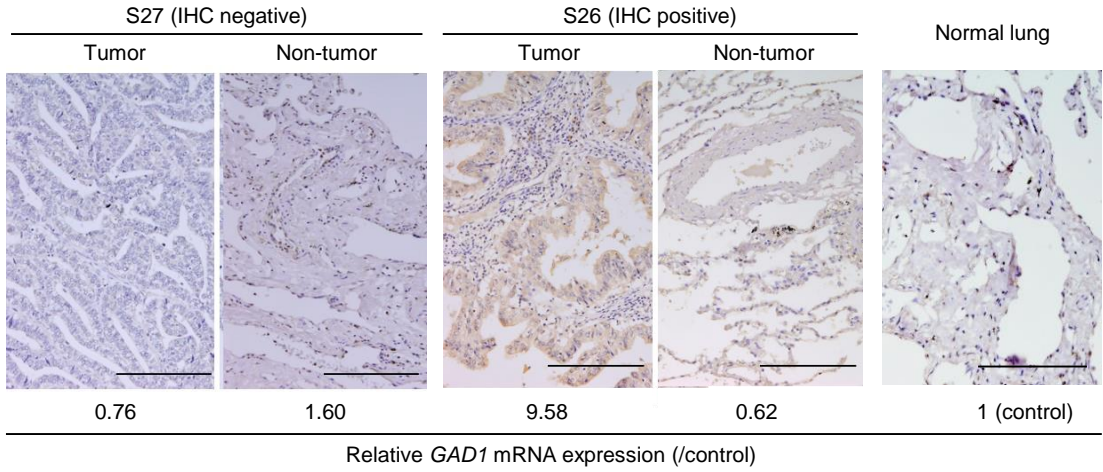
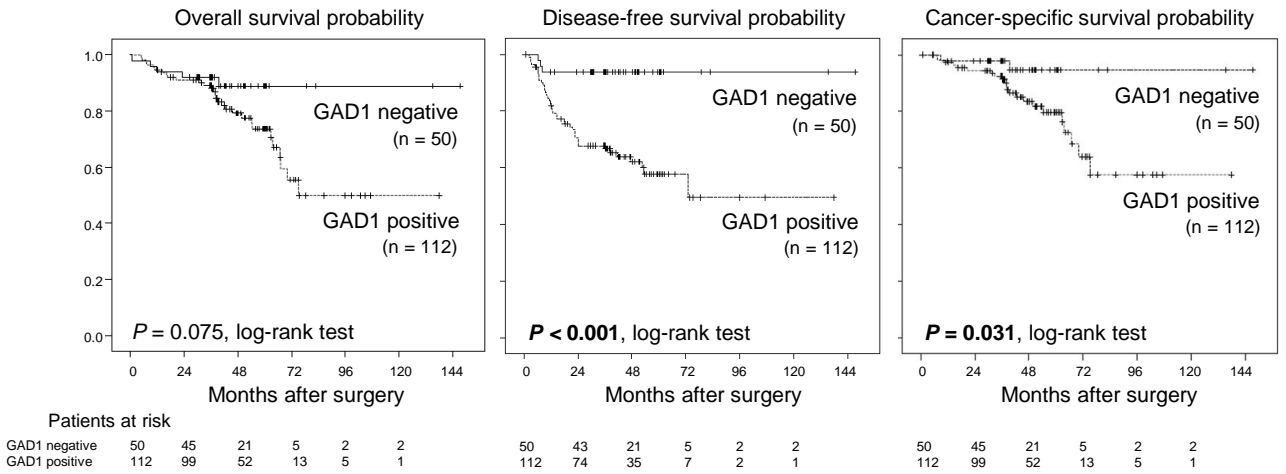


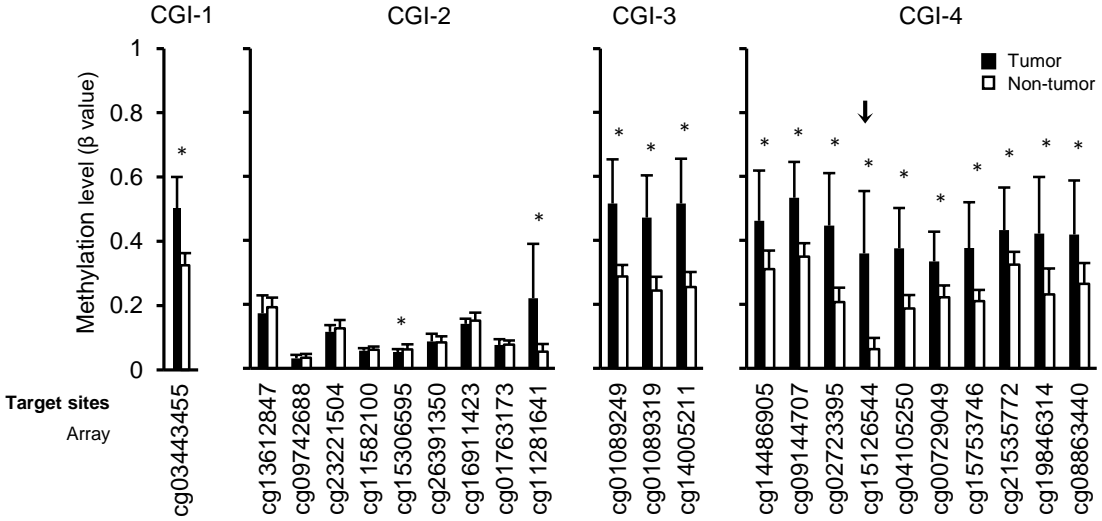
Figure 3

A



B





Supplementary Figure S2

